ii) compare averaged thickness of next two succeeding beds with preceding one (1 = thicker; 0 = thinner) [two bed moving average after Heller & Dickinson (1985)] used for the identification of upward thickening and upward thinning bed cycles

Both RAM and RUD calculations were carried out.

Davis (1986), Reading (1996), Murray *et al.* (1996) and Chen & Hiscott (1999a) discuss the common pitfalls in the application of statistical analysis and this study is sensitive to their comments when interpreting the results

2 CHARACTERISATION OF LOBE DEPOSITS IN OUTCROP: E-FAN, CINGÖZ FORMATION, S-TURKEY

2.1 Geological background

2.1.1 Location and setting

The Miocene Cingöz Formation forms part of the thick Tertiary infill of the southern Turkish Adana Basin in a tectonically complex collisional setting. The basin is bound by the Ecemiş Fault Zone in the west, the Misis Structural High in the southeast and the overthrust Tauride Orogenic Belt in the north (Williams *et al*. 1995; fig. 2.1). The basin forms the northern part of the greater Çukurova Basin, separated from its southern part, the Iskenderum Basin, by the NE-SW trending Misis Structural High (Kelling *et al*. 1987). The Çukurova Basin extends submarine to Cyprus as the Cilicia-Adana Basin (Williams *et al*. 1995).

The Çukurova Basin is located entirely on the Anatolian Plate (Williams *et al*. 1995) above the zone of Cenozoic suturing between the Afro-Arabian and the Euro-Asian plates (Sengör & Yilmaz 1981; Dewey *et al*. 1986). The age of the plate collision is not established, various authors assigning different ages to it: Late Cenozoic (Kelling *et al*. 1987), Early Miocene (Jackson & McKenzie 1984), Middle Miocene (Sengör 1979) and has most recently suggested to be of Eocene to Miocene age (Hempton 1982; Yilmaz 1993).

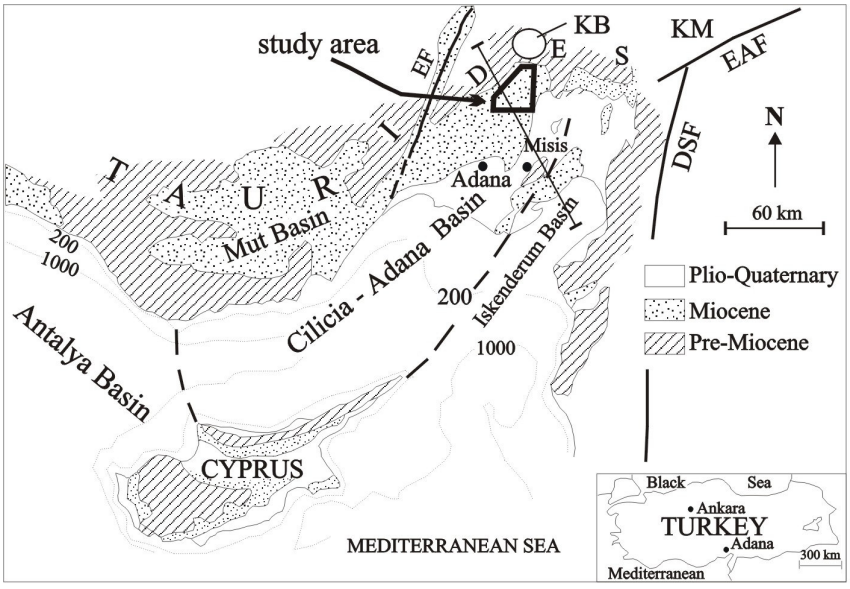

Figure 2.1: Map for the northeastern Mediterranean region showing the general geological setting and the main localities: DSF = Dead Sea Fault; EAF = East Anatolian Fault, EF = Ecemis Fault zone; KB = Karsanti Basin; KM = Kharamanmaras (from Yetis *et al.* 1995). Box: location of study area. Line: NNW-SSE cross-section of figure 2.2.

The structural evolution of SE Turkey is controlled by the interaction of several major wrench faults in the Kahraman Maraş triple junction (fig. 2.1), the N-S trending Dead Sea fault zone (Africa-Arabia), the NE-SW trending Bitlis Suture (Arabia-Eurasia) and the eastern part of the Hellenic Trench (Africa subducted under Eurasia) (Williams *et al*. 1995). The Adana Basin is thought to have formed as a result of the incompatibility problems arising at this triple junction (Hempton 1982; Robertson 1998). Gökçen *et al*. (1988) suggest that the basin originated as a perisutural foreland basin which subsequently developed into a transpressional basin

complex related to the creation of the Kahraman Maraş continental triple junction (Sengör *et al*. 1985; Görür 1992; Ünlügenç 1993). A variety of other basin types have been suggested to fit the observed tectonic and sedimentary configuration of the Adana Basin, they include fore-arc basin (Aktaş & Robertson 1984; Aksu *et al*. 1992; Görür 1992), extensional fore-arc basin (Jackson & McKenzie 1984), back-arc basin (Floyd *et al*. 1992), foreland basin (Kelling *et al*. 1987; Williams *et al*. 1995) and a flake and plate triple junction compatibility basin (Dewey *et al*. 1986).
In the Adana Basin, the basement units, consisting of an ophiolite complex and Palaeozoic and Mesozoic rocks, are unconformably overlain by an approximately 6000 m thick Cenozoic succession (fig. 2.2; Yetiş & Demirkol 1986; Görür 1992). No *in situ* Palaeocene and Eocene rocks are known. The Cenozoic sedimentation appears to begin with a group of redbeds of Oligocene age best developed in the Karsanti Basin, immediately north of the Adana Basin (Ünlügenç *et al*. 1992). Today, Tertiary units outcrop mainly in the northern part of the basin, whereas Quaternary deposits are exposed on its southern side (fig. 2.1). Generally, the Tertiary deposits exhibit complex lateral and vertical facies relationships (Yetiş *et al*. 1995).

2.1.2 Tectono-sedimentary evolution and stratigraphy of the Adana Basin

The initiation of the Adana Basin probably took place after the late Eocene to Oligocene trust emplacement of an ophiolitic complex in the Taurides to the north of the basin (Williams *et al*. 1995; fig. 2.3). The formation of the foredeep was probably caused by southward compression and thrusting (Williams *et al*. 1995) or regional crustal extension and detachment faulting (Karig & Kozlu 1990). Robertson (1998) proposes a combination of these effects suggesting that regional convergence was partially adsorbed by crustal shortening to the north, and subduction 'roll-back' to the south, thus explaining why the Adana Basin shows some features akin to a foreland basin but without evidence of a preserved thrust load.

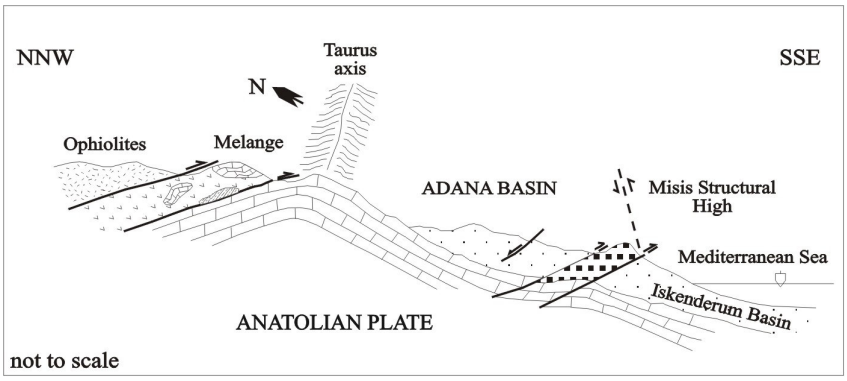

Figure 2.2: Generalised structural cross-section across the Adana Basin, Misis Complex and Iskenderum Basin (from Ünlügenç 1993). Location of cross-section marked in figure 2.1.

The Cenozoic development of the Adana Basin can be subdivided into an upward succession of pre-transgressive, transgressive and regressive character (Yetiş *et al*. 1995) which roughly corresponds to megasequences identified by Williams *et al*. (1995) (fig. 2.4). These megasequences are separated by distinct sequence boundaries visible in the subsurface data.
In the Eocene, ophiolitic thrust sheets were obducted in a southerly direction, thereby overriding an ophiolitic melange (fig. 2.3). During the early Oligocene, erosion and planation of these thrust sheets took place. In the late Oligocene extensional faulting in the north of the region occurred creating major half-graben settings (Williams *et al*. 1995; Robertson 1998). This was controlled by deep-rooted basement faults that cut and displaced the thin-skinned ophiolitic thrust sheets. In these half-grabens continental sediments were deposited, the alluvial to lagoonal redbeds of the **Karsanti Formation** and the alluvial to coastal **Gildirli Formation**. They form the pre-transgressive deposits of Yetiş *et al*. (1995) (fig. 2.3; 2.4). The Karsanti Formation is dominantly exposed in the Karsanti Basin.
Following a regionally extensive phase of tectonic compression, a major marine transgression commenced in the late Oligocene in northern Cyprus and in the early Miocene in adjacent southern Turkey. During this time, continental deposition continued only in the area of the Ecemiş Fault Zone (Yetiş *et al*. 1995).
In the Miocene (Aquitanian and Burdigalian) minor extensional faulting occurred which William *et al.* (1995) believe to result from renewed thrust activity in the Taurides to the north. Robertson (1998), however, suggests regional extension originating to the south to be responsible. During this time reef growth began on the top of fault blocks (**Karaisali Formation**; fig. 2.3).

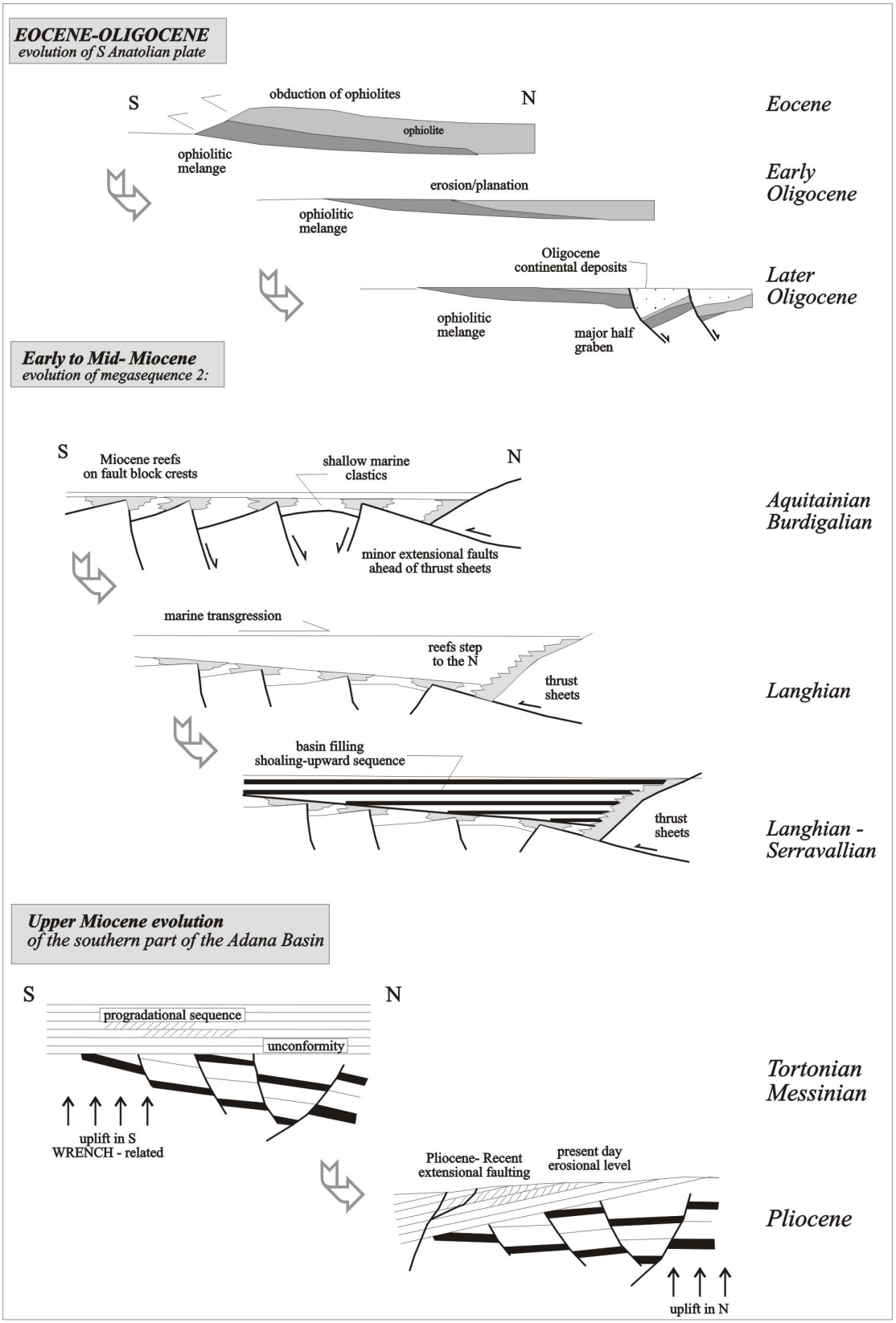

Figure 2.3: Eocene to mid-Miocene evolution of the northern Adana Basin and upper Miocene evolution of the southern Adana Basin (redrawn from Williams *et al.* 1995).

The continued deepening generated a deep underfilled basin. The relatively high sea level of this transgressive phase caused the northward migration of the carbonate reefs (**Karaisali Formation**) (Williams *et al*. 1995; Yetiş *et al*. 1995; Robertson 1998). The shallow marine, fossiliferous clastic deposits of the **Kaplankaya Formation** are associated with the reefal and slope environment (Görür 1979, 1992; Yetiş & Demirkol 1986; Nazik & Gürbüz 1992; Gürbüz 1993).

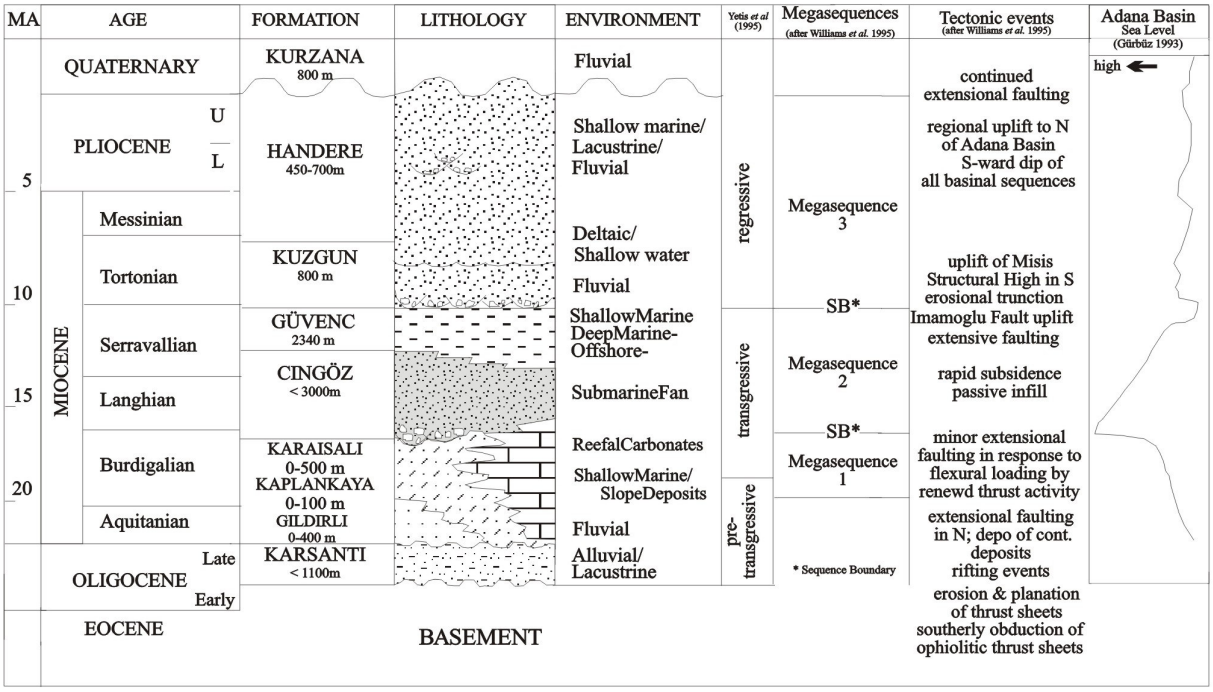

Figure 2.4: Generalised stratigraphic columns of the Adana and Karsanti Basin. Compiled from Nazik & Gürbüz (1992), Gürbüz (1993), Yetis *et al.* (1995) and Williams *et al.* (1995). Gürbüz (1993) used time scale of Harland *et al.* (1990), other authors put the Langhian age from 16.5 to 15 MA (Robertson 1998) or 21.5 - 20 MA and a top Serravallian age of 15 MA (Haq *et al.* 1987a).

The basin is then filled with a shoaling upward sequence of turbidites (**Cingöz Formation**) and deep marine basinal shales (**Güvenç Formation**) during late Burdigalian, Langhian and Serravallian times (Ünlügenç *et al*. 1992; Gürbüz 1993). The deep-water clastic system shows no syntectonic sedimentation effects in seismic profile. Its seismic character reveals aggradation consistent with the passive infill of an underfilled foreland basin (Ünlügenç *et al*. 1992; Williams *et al*. 1995). The geometric and stratigraphic facies relationships are very complex. The **Cingöz Formation** is partly coeval with and partly superimposed on the **Kaplankaya, Karaisali** (both: Burdigalian-early Serravallian: Yetiş 1988) and **Güvenç Formations** (Burdigalian-Serravallian: Özelik 1993) (Yetiş *et al*. 1995) largely representing lateral facies variations of each other passing from the subaerial alluvial facies of the **Gildirli Formation** to alluvial fan, fan delta and shallow marine facies of the **Karaisali** and **Kaplankaya Formation** in to deep-marine facies of the **Cingöz** and **Güvenç Formation** (Satur 1999). The latter is younger in its upper units, transgressing over the **Cingöz Formation** during late Serravallian (fig. 2.4).

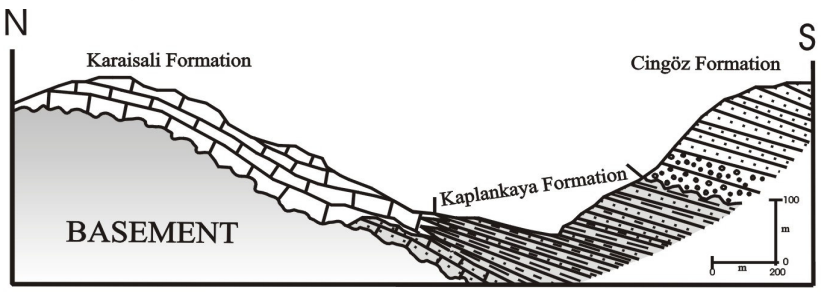

Figure 2.5: Schematised geometric and stratigraphic relationship between the basement rocks, the Karaisali, Kaplankaya and Cingöz Formation in the northern Adana Basin from Gürbüz (1993), modified after Yetiş & Demirkol (1986).

Figure 2.5 shows a cross-section through the northern Adana Basin displaying the lateral and vertical relationships in a simplified manner. The deeper marine Miocene facies persisted longer in the Misis area and in northern Cyprus than in the Adana Basin (Yetiş *et al*. 1995). The above formations form the

transgressive units after Yetiş *et al*. (1995), and based on their seismic character, the first two megasequences of Williams *et al*. (1995; fig. 2.4).
During the Late Miocene (Tortonian to Messinian) the uplift of the Misis Structural High in the south caused erosion of the basin fill prior to the deposition of continental deposits. The shallow marine and terrestrial clastics of the **Kuzgun Formation** and the predominantly fluvial **Handere Formation** reflect the shoaling of the basin (third megasequence of Williams *et al*. 1995). The Imamoglu Fault Zone to the east is reactivated as a positive flower structure during and after the deposition of continental deposits (Sengör & Yilmaz 1981; Kelling *et al*. 1987; Karig & Kozlu 1990).
Later, regional uplift to the north of the basin generates a 15 - 20^{o} southern dip on all basinal sequences resulting in the present day geometry of the basin (fig. 2.3).
The relative sea-level curve (fig. 2.4), which Gürbüz (1993) constructed for the Tertiary of the Adana Basin closely mirrors the Cypres and global sea-level curves of Robertson *et al*. (1991) and Haq *et al*. (1987a,b) respectively suggesting that the Cingöz Formation was deposited during regression which continued into the late Serravallian. However, Yetiş *et al*. (1995) more detailed analysis of the Neogene infill of the Adana Basin suggests that the Cingöz Formation was in fact deposited during gradually rising sea level, spanning from the lowstand of the alluvial to coastal Gildirli Formation to the highstand of the deep-marine Güvenç Formation (Satur 1999).

2.2 The Cingöz Formation

Traditionally, the Cingöz Formation is subdivided into 3 members: the conglomeratic Ayva Member, the sandstone-shale Topalli Member and the shale-dominated Köpekli Member (Schmidt 1961). Görür (1977) interpreted the Ayva Member to represent proximal and the Topalli Member to be distal turbidites. Yetiş & Demirkol (1986) later assigned the Köpekli Member to the Güvenç Formation. This study does not employ these local stratigraphic subdivisions but uses generic deep-water clastic terminology for a more general approach. Yetiş & Demirkol (1986) and Yetiş (1988) recognised the Cingöz Formation to consist of two sandy lobes within the Güvenç Formation which Ünlügenç *et al.* (1992) interpreted to be submarine fan deposits (fig. 2.6). Gürbüz (1993) and Gürbüz & Kelling (1993) acknowledged them to be two small, laterally coalescing submarine fan systems, which were deposited in a rapidly subsiding basin during late Burdigalian to early Serravallian times (fig. 2.7; Nazik & Gürbüz 1992). The Cingöz System was active for approximately 2.7 myr during which approximately 3000 m of sediments were deposited (Gürbüz 1993). Foraminiferal dating reveals an latest early to middle Miocene age (Praeorbulina glomerosa curva, Orbulina suturalis and Globorotalia mayeri zones / foraminiferal biozones PN8 – PN11), while calcareous nanoplanktons disclose an early-middle Miocene age (Sphenolithus leterorphus Zone [NN5]) to middle Miocene age (Discoaster exilis Zone [NN6]) (Toker *et al.* 1998). The Cingöz system is interpreted to have been deposited under temperate conditions with water temperatures gradually becoming colder due to influx of cold-water currents (Demircan & Toker 1998).
The Cingöz Formation extends from the Karaisali-Gildirli Line in the west to Memişli in the east and southeast (fig. 2.6), where its development is restricted by a probable structural high, the Imamoglu Fault Zone (Kelling *et al.* 1987). The total exposed area amounts to ~ 900 km^2. Seismic and borehole data [Gilbaş 2 Well: N 37°13'15"; E 35°25'28"] reveal the subcrop presence of approximately 1640 m of Cingöz deposits, overlain by 1190 m of basin plain sediments approximately 20 km southeast of Çatalan village (Naz *et al.* 1991; *pers. comm.* Naz 1997). The total southern extent is unknown. Seismic profiles present an aggradational character (Williams *et al.* 1995). Extensional faulting in the north and northwest (NE-SW and ENE-WSW trending faults) and in the northeast (NW-SE to NNW-SSE trending faults) is commonly observed, particularly throughout the northern Cingöz Formation (Ünlügenç 1993). Based on seismic data, Ünlügenç (1993) demonstrates that extensional events of three different ages have affected the basin fill i) early to mid Miocene, ii) late Miocene and iii) late Pliocene ("neotectonic stage"). However, it is difficult to relate the faulting events recognised in the field to the faults interpreted on seismic sections.
Gürbüz (1993) interpreted the Cingöz Formation to represent an active margin fan complex *sensu* Shanmugam & Moiola (1988) due to its small size, the narrow contemporaneous shelf and coastal zone and the coarse sediment load.

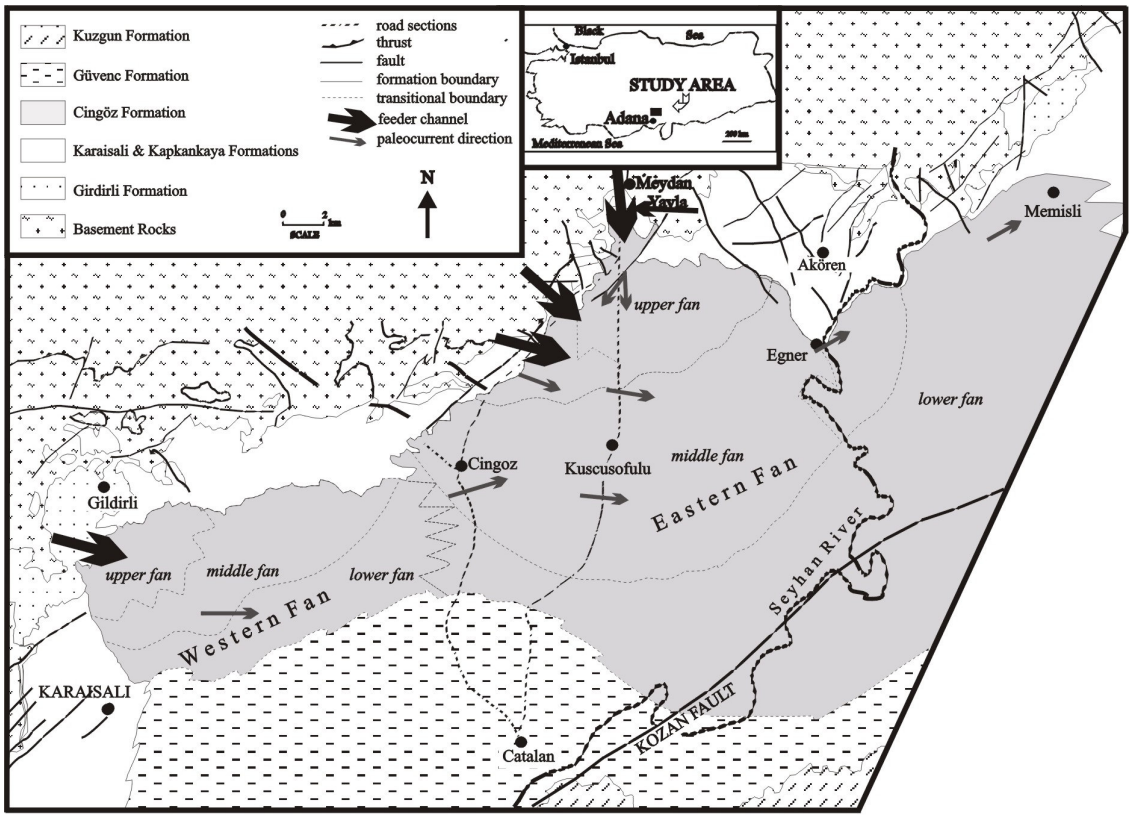

Figure 2.6: Geological map of the northern Adana Basin from Gürbüz (1993), modified after Satur et al. (1997).

2.2.1 The western and eastern fan

The two Cingöz fans, western and eastern fan after Gürbüz (1993), were fed by separate, incised feeder systems conveying gravel and sand from the adjacent, actively uplifted areas of the Tauride Orogenic belt, across a narrow (~ 3 km wide) carbonate platform (Karaisali Formation) into the basin. The western fan (W-Fan) was fed from the NW and the eastern fan (E-Fan) from the N and W (fig. 2.6; Gürbüz 1993; Satur 1999).

Both fans exhibit conglomeratic feeder-channel complexes, and into thick successions of turbidite sandstone and shale alternations in the basin (Görür 1977; Gürbüz 1993; Yetiş *et al.* 1995). But despite their contemporaneous deposition and some similarities, the development of the two adjacent fan systems differs (table 2.1).

The W-Fan is fed by one large feeder system which records a succession from alluvial fan and fan delta to deep marine sediments. The overall development is structurally and topographically controlled, showing a strong west-east confinement (Satur 1999). This conduit displays multiple phases of infilling indicating pulses of sediment supply. Apart from channel and lobe elements (Gürbüz 1993), non-erosional tongue-like sediment bodies were identified to be a major component of this fan system (Satur 1999).

The E-Fan is sourced by at least 4 feeder channels (fig 2.6: 3 main and 1 tributary feeders). These channels display multiple phases of infilling indicate initial deposition from fan deltas passing upward into non-channelized, sandy deeper water turbidites (Satur *et al.* 1997; Kostrewa *et al.* 1997; Satur 1999).

Gürbüz (1993) showed that at the early stage of the Cingöz system the western and eastern fan formed separate entities in late Burdigalian to early Langhian times. Western Fan progradation resulted in interfingering deposition during Langhian-Serravallian times (fig. 2.7) before retreating and their subsequent separation during the final stages of their development (late Serravallian). Satur (1999), however, believes W-Fan deposition to begin later and end earlier than the E-Fan one (table 2.1).

	WESTERN FAN	EASTERN FAN
Areal extent	~ 150 km^2 exposed, eastern and subsurface extent unknown	~ 750 km^2 exposed, southward subsurface extension at least 20 km
Stratigraphic thickness	maximum thickness around 1500m	maximum thickness around 3000 m
Feeder system	one sand-rich fairway	one main feeder and 3 tributary channels
Grain size	coarser at base	relatively less conglomeratic
Sequences	2 main megasequences	at least 8 (thinner) megasequences
Source and transport direction	sourced from NW ; transport towards SE	sourced from N, NW, W; transport towards SW in lower part, deflected to ENE in upper part
Development	lower stacked channel sequence and upper lobe dominated sequence, gradually passing upward into outer fan/basin plain but with some small channels and lobes	thick basal sequence of isolated channels, followed by lobes; during a second phase, small channel sequence followed by succession of lobe-dominated 'midfan' sequences
Time of activity (Nazik & Gürbüz 1992) *	late Burdigalian – Serravallian	late Burdigalian - Serravallian
Fan system after Mutti (1985a) through time (Toker *et al.* 1998; Satur 1999)*	1) absent (lower Langhian) 2) Type I: bulk sand depositon in channel-detached lobes 3) Type II: bulk sand deposition in channel- attached lobes and channel-fill sequences 4) absent (upper Serravallian)	1) Type I 2) Type II 3) Type II 4) Type III: channel-levee complex without lobes
Structural control	channel confinement; restriction to west basement structure to south	channel confinement; restriction to east by a probably structural barrier, shallowing to east
System tract after Posamentier *et al.* (1988)$^{++}$	lowstand to transgressive / highstand system tract	lowstand to transgressive / highstand system tract
Ichnofossil assemblages	Cruziana	Mixed and Nereites
Environmental conditions	eutrophic (high organic productivity)	oligotrophic (low organic productivity)
Bathymetry	shallower (sublitoral zone; ~ 200m water depth)	relatively deeper (abyssal; (500) to > 2000 m water depth)

Table 2.1: Main features of the western and eastern submarine fans, compiled after Naz *et al.* (1991), Gürbüz (1993), Ünlügenç (1993), Toker *et al.* (1998), Demircan & Toker (1998) and $^{++}$Satur (1999).

Petrographic studies of the conglomerates, the coarse- and medium-grained sandstones reveal subtle differences in the composition of the different fans reflecting their respective source areas (table 2.1 ; Naz *et al.* 1991; Gürbüz & Kelling 1993; Gürbüz 1993). This was confirmed by a recent geochemical pilot study (Satur 1999). The Early Cenozoic fold-thrust belt to the north of the basin with incorporated ophiolite bodies and magmatic arc rocks forms the major source (Gürbüz & Kelling 1993; Gürbüz 1993). Cronin *et al.* (2000) identified mixed siliclastic carbonaceous turbidites to be prominent clope to the slope margin.
W-Fan deposits accumulated to approximately 1500 m (table 2.1) while the E-Fan thickness amounts to 2500 m (Gürbüz 1993; fig. 2.8). It is thought that local basement topography, possibly created by local tectonics, played a major factor controlling the differences in dimension and thickness observed (fig. 2.9).

*Note the differing ages given for the inception of the Cingöz deep-water clastic system based on either foraminiferal (Nazik & Gürbüz 1992) or nanoplankton (Toker *et al.* 1998) dating. Satur (1999) utilises the nannoplankton biostratigrahpy, while other workers in the Adana Basin prefer the foraminiferal-based biostratigraphy (e.g. Gürbüz & Kelling 1993; Gürbüz 1993; Yetiş *et al.* 1995; Cronin *et al.* 2000; this study).

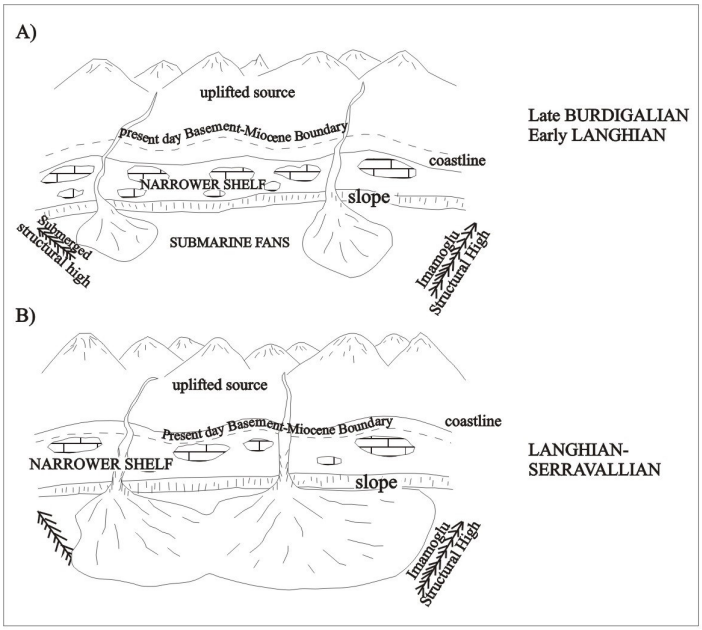

Figure 2.7: Schematic diagram showing the evolution of the Cingöz submarine fans in the northern part of the Adana Basin (from Gürbüz 1993).

Different rates of subsidence within the receiving basin sectors must have allowed these gross thickness changes and different accumulation rates in the same time interval (Gürbüz 1993; Ünlügenç 1993; Kostrewa *et al.* 1997).

Local topography further played a role in influencing the development of the individual systems. The prevalent transport direction of the W-Fan is towards the SE-E and remnants of Palaeozoic and Mesozoic rock to the W and SW (west of Karaisali) suggest a topographic high limiting growth towards this direction (Gürbüz 1993; fig. 2.6). Satur (1999) found a palaeotopographic high to the south to be responsible for the distinct, elongate W-E trend of the system. The extent of the E-Fan is restricted to the east and SE by a probable structural high, the Imamoglu Fault, with strike-slip character, which was active during the Miocene (Williams *et al.* 1995). Sedimentological evidence like facies variations and contrasting palaeocurrents further support this (Gürbüz & Kelling 1993; Gürbüz 1993). On this structural high, shallow marine sediments accumulated with occasional slumping directed to the SW (fig. 2.1).

Trace fossil assemblages are diverse and abundant. The W-Fan is marked by the Cruziana ichnofacies which indicates eutrophic, well oxygenated and shallower water conditions. Seilacher (1967) and Frey & Pemberton (1984) assign this ichnofacies to the sublitoral zone, to 0-200 m water depth. The E-Fan contains mixed and Nereites ichnofacies assemblages indicating oligotrophic, less oxygenated, probably more restricted and relatively deeper water environments (table 2.1; Demircan & Toker 1998), which increased during deposition (Satur 1999).

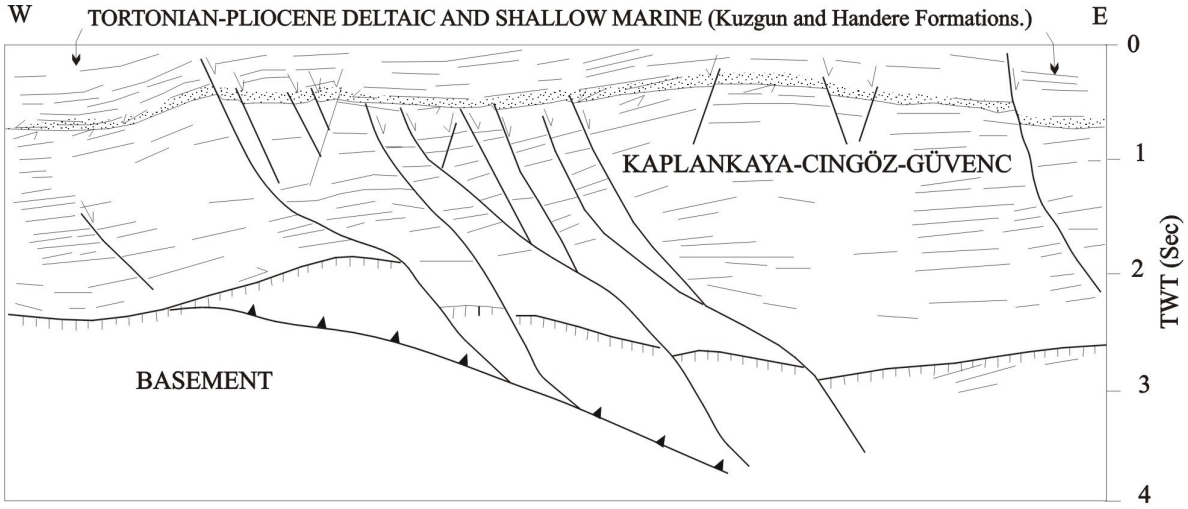

Figure 2.9: An interpreted seismic W-E line through the Kaplankaya, Cingöz and Güvenç Formations forming megasequence 2. It shows an aggradational nature of the reflectors and erosional truncations beneath megasequence 3 (top) in the west and central part of the line. Extensional faults with easterly component of downthrow are present (from Williams *et al.* 1995).

The Cingöz Formation is comprised of numerous vertically stacked, aggrading and prograding intervals formed during late Burdigalian - Serravallian age (Naz *et al.* 1991), which Satur‘s (1999) analysis of the channel-fill sequences of both the western and eastern fan confirmed. This study further supports these

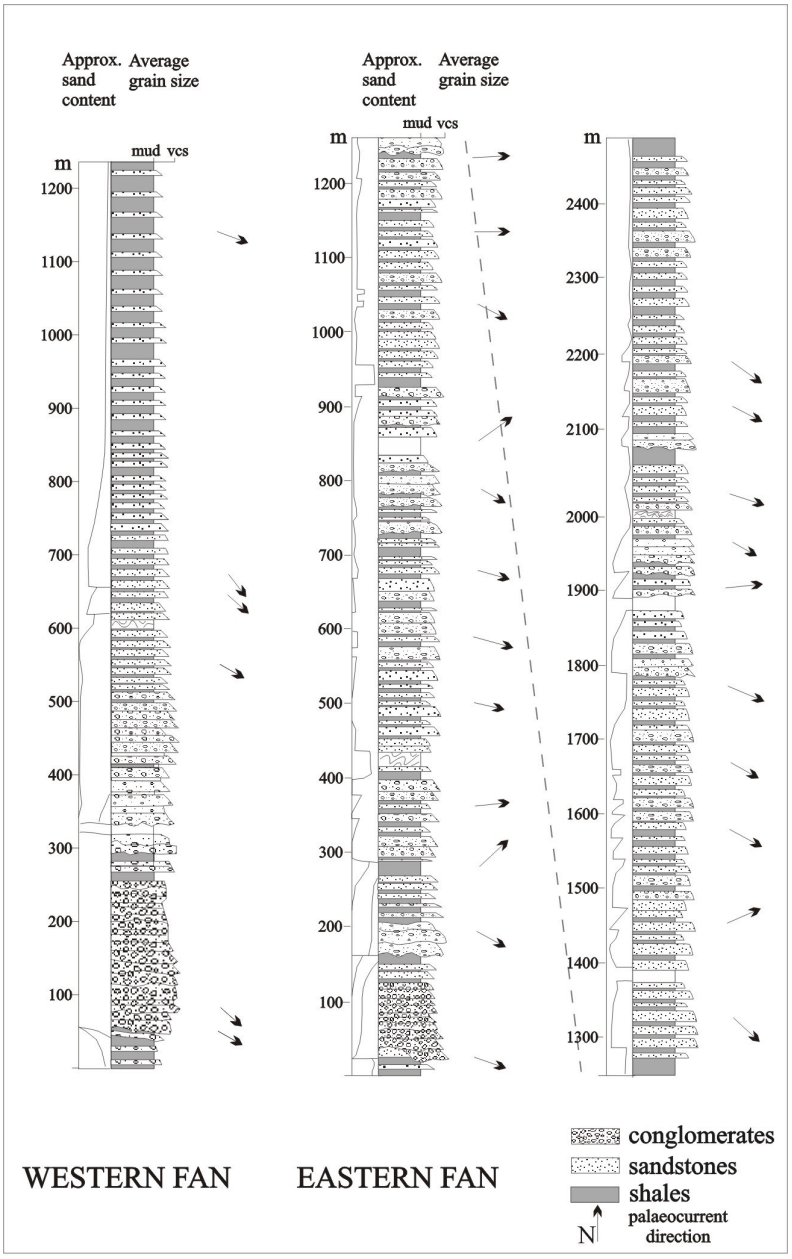

Figure 2.8: General logs through the western and eastern fan, Cingöz Formation (from Gürbüz 1993).

findings based on the analysis of the sandy non-channelized fan deposits of the E-Fan system (*chapter 2.4*). But while Naz *et al.* (1991) and Gürbüz (1993) suggest the Cingöz Formation to be an example of a typical lowstand fan system, Yetiş *et al.* (1995) and Satur (1999) believe the Cingöz Formation to be a good example of a fan system developping during a transgressive phase where local tectonics, the basin configuration and sediment supply are thought to have a fundamental influence on the development (Gürbüz 1993; Ünlügenç 1993).

Satur (1999) recently suggested to refer to the eastern and western fan of the Cingöz Formation as eastern and western area of a single Cingöz fan system, which are characterised by different depositional styles. However, this study retains the old names "eastern fan" and "western fan" which are compatible to the eastern and western area of Satur (1999).

2.2.2 Eastern fan framework

The eastern fan (E-Fan) is the larger of the two Cingöz fan systems. The total exposed area is approximately 750 km^2. It reaches from Cingöz in the west to Memişli in the east (fig. 2.6). The deposits in the far NE are believed to be of shallower origin (Ünlügenç 1993).

This fan has been the object of numerous investigations because of its well exposed and reasonably accessible channel-fill deposits. Recent studies include Gürbüz & Kelling (1993: provenance studies), Gürbüz (1993: palaeogeography, sedimentology, biostratigraphy), Ünlügenç (1993: regional and structural geology), Satur *et al.* (1997, 2000) and Satur (1999: proximal, channelized facies), Kostrewa *et al.* (1997: proximal and distal sandy, non-channelized facies) and Demircan & Toker (1998: trace fossil assemblages, palaeoenvironment) and Nazik & Gürbüz (1992) and Toker *et al.* (1998: biostratigraphy).

This study focuses on the primarily non-channelized sandy turbidites exposed in the northern and central fan area (fig. 2.10), their sedimentological character, their basic building blocks and subenvironments, and factors controlling their development. This necessitated a revision of the fan-framework to put the observed relationships into a new, improved context.

2.2.2.1 Feeder channel systems

Previous studies suggested that the E-Fan was a single-sourced system with approximately 500 m of channel-fill deposits preserved (Gürbüz & Kelling 1993; Gürbüz 1993; *pers. comm.* Gürbüz 1996). Satur *et al.* 1997) and Satur (1999) investigated the spatial and temporal changes in facies and architecture of the proximal, channelized E-Fan. They found the fan to be sourced by at least 4 feeder channels (fig. 2.10). The north-south trending bypass channel 1 is the main feeder channel. Tributary channel 2 in the east believed to have been a shorter-lived subsidiary to the main channel (Satur 1999). Channels 3 and 4, which trend northwest-southeast and west-east respectively, are located at the northwestern margin (fig. 2.10).

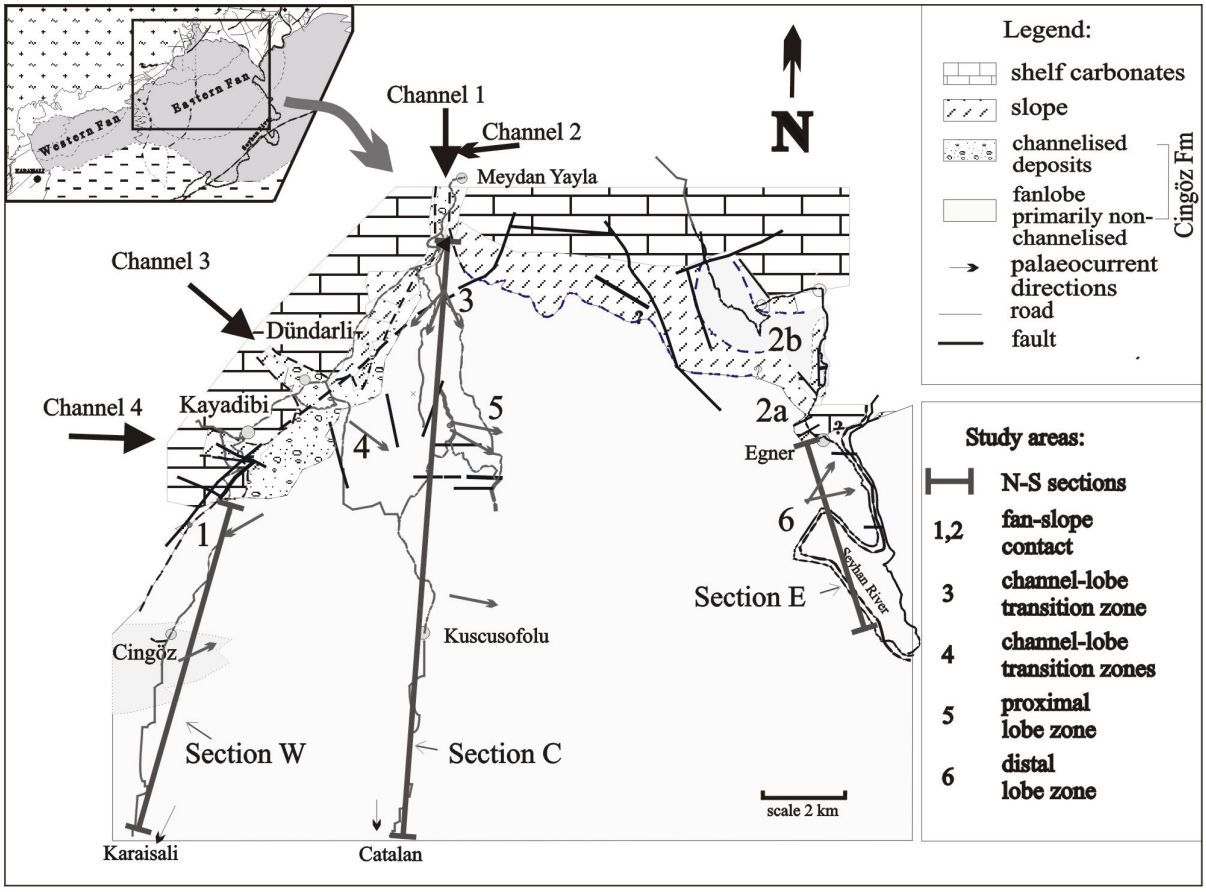

Figure 2.10: Geological map of the central and northern part of the exposed E-Fan and adjacent formations with location of key study areas (after Satur *et al.* 1997, Kostrewa *et al.* 1997, Gürbüz 1993 and Ünlügenç 1993).

Channels 1, 3 and 4 appear to be structurally controlled and the facies point to deposition from fan deltas that pass upward into deeper water turbidites. The channel 1 and 3 have similar clast lithologies, while channel 4 shows a discretely different lithology. A confluence area in the north-west suggests channels 1 - 3 to be partly coeval, while channel 4 became active at a later stage, partly eroding into and reworking channel 3 deposits (Satur 1999). The channel-fill of channel 1 records a mixed system where initial erosion is followed by a period of low sedimentation and deposition of clastic sheets. In a lateral, downcurrent direction, variations in the internal architecture and channel-floor gradient within a seven km depositional-dip section of channel 1 records changes in the hydraulic conditions with complex inter-relationship between the flow turbulence, erosion, gradient and confinement of the turbidity currents.
The channels range in size from 45 – 600 m in width and between 6 – 90 m in thickness of channel-fill deposits are preserved (Satur 1999). They pass upward into thick, sandy, predominantly non-channelized lobe deposits (Gürbüz 1993; Kostrewa *et al.* 1997; plate 2.1).

2.2.2.2 Facies distribution and architecture of the non-channelized E-Fan sections

Three overview logs were taken (table 2.2), recording the E-Fan deposits from the gravelly channel-fill and/or fan-slope contact in the north to the younger fan fringe sediments in a basinward direction to the south. They record the downcurrent as well as lateral development of the E-Fan sandy basin infill. Together with other study areas (fig 2.10; NW: transition channelized - non-channelized, WNW and NE: fan-slope relationship) and the detailed sedimentological study of various lobe depositional environments located in different fan positions (chapter 2.4), they provide the framework for understanding the development of the fan system. Additionally, data collected in other studies (Gürbüz 1993; Satur *et al.* 1997; Satur 1999) is utilised as indicated (fig. 2.11). The zone of interfingering between the eastern and western fan, which is exposed around Cingöz village (fig. 2.10), is included in this study.
Relogging of major parts of the E-Fan, with emphasis on the sand-dominated proximal to mid-section areas, has revealed that the total fan thickness is 3700 m in the central section of the E-Fan. This is considerably thicker than previously recorded (e.g. 2500 m of Gürbüz 1993). However, marked thickness variations (table 2.2; fig. 2.11) are present from west to east as well as distinctly changing lithofacies associations, suggesting a more complex development of the fan system then previously interpreted. The deposits show little to no deformation. Faulting is abundant, mostly of unknown vertical and/or lateral displacement (Ünlügenç 1993; this study).

SECTION	THICKNESS	N-S EXTEND	BEGINNING	END
Section W (west)	1700 m	fan - slope to fan – basin plain contact	N 37 24'20'' E 035 16'53'	N 37 16'29'' E 035 16'17''
Section C (central)	3700 m	channel-fill to fan - basin plain contact	N 37 28'48'' E 035 20'37''	N 37 18'20'' E 035 17'58''
Section E (east)	870 m	fan - slope to distal fan fringe; stratigraphic top of fan not exposed	N 37 25'20'' E 035 26'20''	N 37 23'00'' E 035 27'10''

Table 2.2: Location, thickness and extend of overview logs (fig. 2.10)

Central section (Section C of fig. 2.11):

An overall fining-upward succession from proximal to distal fan deposits comprising channel-fill deposits at its base, passing upward into 100s of metres of thick successions of coarse, thick-bedded sandstones subsequently thinning and fining upward to the fan fringe deposits located in a distal, southward direction.
The central section can be grouped into 7 units of distinctive sedimentological character (fig. 2.11: marked as C1-C7 in section C):

C1) An 80 m thick conglomeratic unit (incised channel 1 fill deposits (Satur *et al.* 1997)) of clast and matrix-supported conglomerates with very little finer-grained material (plate 1.2). The clast lithologies encountered are: basement ophiolites (~ 50%), Karaisali Limestone (~ 40%) and basement sandstone and limestone (~ 10%), with maximum clast sizes reaching 10 m (Karaisali Limestone). Feeder channel 1 is interpreted to have been approximately 600 - 750 m in width (aspect ratios: 7.5 - 9.7) transporting sediments in a SSE-SSW (200/160) direction. Few laterally persistent siltstone beds are present, which are thought to represent periods of quiescence during the channel development.

C2) A 40 m thick debrite, consisting mostly of chaotic, fossiliferous Kaplankaya slope siltstones. Internal deformation and few floating clasts are conspicuous. This unit was previously interpreted to represent slope progradation over temporarily abandoned channel segments (Satur 1999) and valley top-levee shales (Naz *et al.* 1991).
90 m of thin- to medium-bedded, dominantly fine- to medium-grained sandstones forming 2 - 6 m thick, thickening-upward cycles in an overall thickening and coarsening-upward succession (basal deposits: S_3 of Lowe (1982) / T_{a-d} of Bouma (1962) coarsening upward to $S_{1-3}/T_{a,b}$ to T_{b-d} at the top of the section) (plate 1.3). Amalgamation, lensing and pinch-out of beds and smaller sandstone packages over distances of 10 - 15 m are common. Palaeocurrents scatter widely from NE to W transport directions (60 – 270°). These sediments are interpreted to represent channel mouth deposits *sensu* Mutti & Normark (1987). 13 m of channel-related

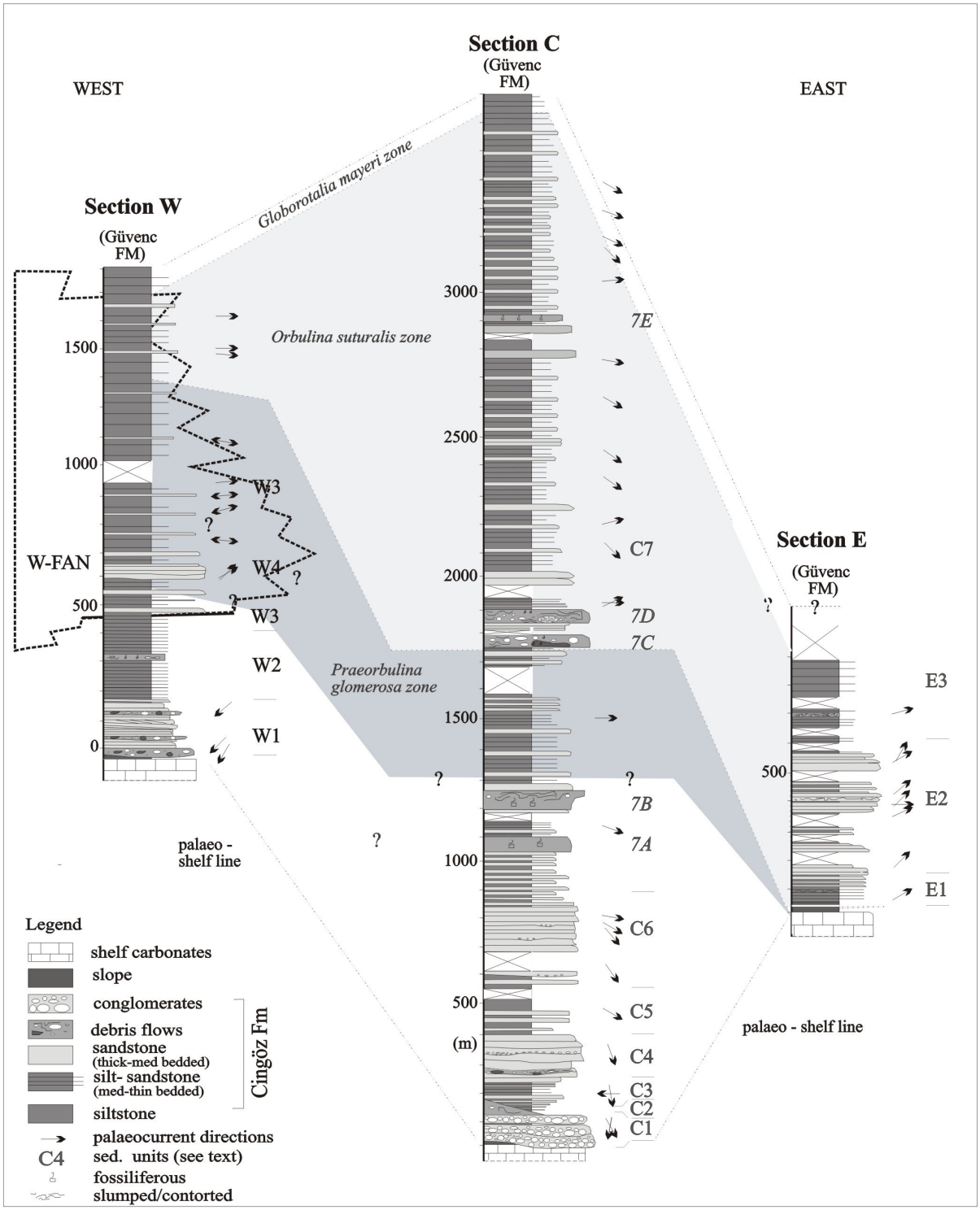

Figure 2.11: General logs through the E-Fan showing the vertical and lateral development within the western, central and eastern sectors. (Biostratigraphic data based on Gürbüz (1993) and Cronin *et al.* (2000); lithological data from Gürbüz (1993): Section W: 850 - 1800 m; Section C: 1900 - 3700 m and from Satur *et al.* (1997): Section C: 0 - 80 m. *7A-E* of Section C represent debris flow deposits referred to in the text.

overbank deposits (Mutti & Normark 1987) consisting of alternating beds of shales and extenisvely current-laminated, fine-grained sandstones (T_{b-e})are intercalated. They are probably located on the edge of a channel (corresponding channel-fill not exposed) with ripple directions pointing towards 210 - 250°, thus approximately 50 - 90° oblique to the main

N-S transport direction. Trace fossils (e.g. Palaeodictyon) and escape burrows are common. This unit was previously interpreted to represent middle fan lobe sequences (Naz *et al.* 1991).

C3) 150 m of laterally extensive, coarse- to very coarse-grained sandstones (S_{1-3}, rarely T_{a-c}), pebbly sandstones, matrix-supported conglomerates (R_1-S_1) and occasional, limestone-rich debris flows (plate 1.3) follow. Channel and lobe elements were identified, organised in subtle fining-upward sequences in an overall fining unit. Palaeocurrents point to a SW - W (210 - 260°) transport direction. This unit represents a channel-lobe transition zone *sensu* Mutti & Normark (1987, 1991; *detailed analysis: chapter 2.4.1*). Previous interpretations include channel-fill deposits (*pers. comm.* Gürbüz 1996) and non-sequential channelized sandstones of the middle fan (Naz *et al.* 1991).

C4) 130 m of typically normally graded, 1 - 35 cm thick, fine- to medium grained sandstones and siltstones (T_{b-e}), interbedded with coarser-grained and thicker-bedded sandstones ($T_{a-d,e}$) and rare pebbly sandstones. The deposits are arranged in 10 – 15 m thick coarsening- and thickening-upward sequences. Overall, a gradual thickening and coarsening of deposits towards the overlying sediments (C6) is present. Palaeocurrents have swung around to a SE (120°) transport direction. These sediments are interpreted to be non-channelized lobe and lobe fringe deposits sourced from feeder channel 1.

C5) 550 m of laterally extensive, predominantly coarse-grained sandstones interbedded with pebbly sandstones and few conglomerates and siltstones (plate 1.4). Deposits are arranged in up to 40 m thick lobe deposits and subordinately in distributary channels and lobe fringe deposits representative of a proximal lobe environment (*detailed analysis: chapter 2.4.2*) This area was sourced from the NW-W (channels 3 and 4) and downcurrent transport directions point to the SE-E. The deposits transitionally pass upward into increasingly thinner-bedded and finer-grained deposits.

C6) The poorly exposed top 2760 m are characterised by fine-grained and thin-bedded sediments interbedded with units of coarser- and thicker-bedded sediments. The uppermost 1200 m are arranged in up to 80 m thick thinning- and fining-upward cycles (Gürbüz 1993).

Coarser units (plate 1.5): typically 4 - 20 m thick, composed of normally graded, parallel-bedded, medium- to coarse-grained sandstone of 0.6 - 1.2 m thickness (S_{2-3},$T_{a-c,d}$). Solemarks such as plumose, flute and/or groove casts are common. Scouring, amalgamation and bioturbation were rarely observed.

Finer units (plate 1.6): composed of regularly bedded, 3 - 8 cm thick very fine to fine sandstone beds (T_{c-d}) interbedded with 3 - 10 cm thick, mostly planar laminated or low angle cross laminated siltstones ($T_{d,e}$). Bioturbation is common. Larger, 1 - 5 m thick fining/thinning- and coarsening/ thickening-upward trends are present, but random trends dominate. Occasionally the deposits are less regularly bedded, displaying greater thickness ranges (1 - 30 cm). The interbedded siltstones are commonly thinner bedded (1 - 3 cm).

The coarser deposits are interpreted to represent lobe deposits (*sensu* Mutti & Ricci Lucchi 1972), while the interbedded fines are associated lobe fringe and/or interlobe deposits (*sensu* Mutti 1977). The contacts between the coarser- and finer-grained units is mostly transitional, resulting in thickening/coarsening- or thinning/fining-upward trends resulting from lobe migration or switching (Bouma 2000). But sharp and/or faulted contacts also exist.

Overall deposits thin and fine towards the top where thin-bedded, shale-rich sediment of the outer fan environment are present (Gürbüz 1993). The palaeocurrent directions indicate a gradual change from SE (130°) in midsection to a predominantly E-ENE direction in the youngest, most distal part.

At least 5 individual debris flows are randomly interbedded (7A-E). They are characterised by a chaotic matrix of fossiliferous siltstones (Kaplankaya slope deposits) and varying proportions of a) well-rounded ophiolitic clasts (Cingöz channel-fill conglomerates), b) limestone clasts (Mesozoic and Tertiary [Karaisali] Formations) and c) shale* clasts. The thickness of these debris flows varies between 7 m (7E) to maximum 80 m (7D) and can be traced laterally for up to 500 m (7D; outcrop limit). Basal contacts are sharp, the often irregular tops are onlapped by overlying deposits (plate 1.6).

* Throughout this study, the term shale (or shales) denotes sediments of clay- to silt grade unless indicated otherwise.

Previous interpretations of the debris flows include "conglomeratic distributary channel-fill deposit in mid-fan position overlain by levee deposits" ('7D'; plate 1.7; Gürbüz 1993). However, the chaotic fabric, internal deformation, squeezed-up shales and deformed sandstone bodies as well as the carbonaceous, shallower-water fossil content of the top siltstone unit with occasional larger, well-rounded floating clasts (plate 2.1), suggest that these deposits represent an unroofing sequences of a) semi-lithified Cingöz channel-fill deposits and b) Kaplankaya slope deposits being subsequently entrained in a debris-flow event.

Debris flows are typically initiated by seismic shock or rapid sedimentation and subsequent slope-oversteepening. Initial sediment failure as slumps or sediment creep may undergo internal deformation and develop into debris flows which can travel far into a basin (Normark *et al.* 1993; Reading 1996). The highly siltstone-rich debris-flow deposits with the entrained well-rounded gravels and large limestone clasts most likely result from a combination of effects such as uplift of the source area, seismic activity and slope failure.

Western section (Section W of fig. 2.11):

Four discrete sedimentary units are present, forming a total of 1700 m of fan sediments (fig. 2.11) encompassing fan-slope contact in the north to basinal shales in the south:

- W_{slope} Karaisali shelfal limestone succeeded by 15 m thick, fault-bounded Kaplankaya slope deposits dominanted by very thinly-bedded, fossiliferous siltstones. Occasional debrites, sliding packages and slump scars are present (*chapter 2.3*).
- W1) 170 m of dominantly medium- to thick-bedded, coarse- to very coarse-grained sandstones (S_{1-3}, $T_{a-c,d}$) interbedded with little silt ($T_{d,e}$) and occasional 1-3 m thick, slope-derived debris flows. Basal fan slope contacts display onlap and infill relationships. (*detailed analysis: chapter 2.3.1*). Lensing, wedging and compensation features are common in the basal sequence.

  The debris-flow deposits (plate 2.2) mainly contain (shelfal-) limestones, deformed clasts of Kaplankaya slope material and a few well-rounded, mostly ophiolitic cobbles in a chaotic, silt-dominated matrix with a high fossil content.

  Towards the east, these deposits can be traced into the coarser-grained central fan deposits. The palaeocurrent pattern points to a W to WSW transport direction indicating a lateral/ marginal position to the main depositional fan area.
- W2) 330 m dominated by a monotonous unit of laterally extensive, typically 5 - 15 cm thick, fine-grained sandstones displaying high sand/shale ratios (4:1; plate 2.3). In its lower part interbedding with occasional thick, coarse sandstones ($S_{2,3}$; T_{a-c}) and up to 1 m thick, limestone clast-rich debris flows are present. These, however, become less common towards the top, where a thick (> 10 m) fossiliferous, silt-dominated debris flow is present (fig. 2.11; plate 2.4; previously interpretated to represent levee deposits: Gürbüz 1993). The palaeocurrent indicators continue to point to a W-SW transport direction. These sediments are interpreted to represent marginal fan deposits (lobe fringe/fan fringe) interbedded with occasional debris flows originating from the basin margin to the north.
- W3) 1100 m characterised by thick, relatively monotone successions of thinner-bedded (5 - 10 cm) and finer-grained sand- and siltstones of distinctly lower sand:silt ratio (2:1). From log metre 450 to 850 thick-bedded, very coarse sediments (unit W4) are frequently interbedded, prior to the monotone succession resuming and finally overlain by basinal shales of the Güvenç Formation. The east-pointing transport directions are in stark contrast to the lower palaeocurrent pattern observed (W2/W3).

  Previous studies (Gürbüz 1993; *pers. comm.* Gürbüz & Kelling 1996) interpreted the deposits to be part of the E-Fan based on the identiefied deeper-water ichnofacies, the somewhat puzzling palaeocurrent patterns are resulting from deflection on a westerly lying submarine high. However, this study proposes the deposits to represent western fan fringe sedimentation within the deepening basin (*discussion*: *chapter 2.5*).
- W4) Over a ca. 400 m thick interval, very coarse-grained sandstones to pebbly gravelstones (plate 2.5, 2.6) (R_3.S_{1-3} of Lowe 1982) alternate with thick units of finely laminated shales ($T_{d,e}$ of Bouma 1962; T_3 of Stow & Shanmugam 1980; plate 2.7). The onset is marked by single or

amalgamated pebbly gravelstone beds (0.6 – 4 m thick) culminating in a 50 m thick package of very coarse, amalgamated deposits (R_{2-3};S_{1-3}) outcropping at Cingöz Village (log metre: 600 – 650). The eastward-pointing palaeocurrent pattern and the markedly strong resemblance to W-Fan deposits located approximately 2 km to the west (this study, Gürbüz 1993) underline its western source. These coarse sediments appear to represent phases of progradation of the W-Fan in form of non-erosive sand tongues *sensu* Satur (1999) into an area otherwise receiving fan fringe sedimentation.

Eastern section (Section E of fig. 2.11)

870 m of fan sediments are exposed, encompassing the fan-slope contact in the north to distal turbidites in a basinal setting in the south. The stratigraphic top is not exposed. Abundant faulting and locally deep erosion by Quaternary fluvial gravels obscure parts of the section.
Three distinct sedimentary fan units are present (fig. 2.11):

E_{slope} A basal thick succession of monotonously thin-bedded, fossiliferous siltstones of Kaplankaya slope deposits. Low angle unconformities within suggest synsedimentary sliding of slope material. A red marker horizon within the Kaplankaya slope deposits, 8 m below the onlap surface of turbiditic fan sediments, dates as the late Burdigalian - Langhian boundary (Cronin *et al.* 2000).

E1) 40 m dominated by thin-bedded (1-6 cm) siltstones alternating with 1 - 3 cm thick very fine to fine-grained sandstones ($T_{c-d,e}$). Trace fossils and plant debris are abundant and up to 1 m thick slumped units are common. The basal 26 m are relatively monotone, then a noticeable upward increase in the sand/shale ratio is recorded by the presence of increasingly thicker-bedded and coarser-grained sandstones ($T_{c-d,e}$), forming isolated, up to 3 m thick sandstone packages. Laterally, the individual sandstone beds display a distinct thinning towards the slope, onlapping it with a low angle contact (*detailed analysis: chapter 2.2.1*), while thickening towards the basinal direction. These deposits are interpreted to represent marginal fan and lobe deposits.

E2) The bulk of the section is formed by a 720 m thick sand-dominated unit characterised by up to 40 m thick discrete sandstone packages displaying very high sand/shale ratios (10:1). They are dominantly composed of laterally extensive, parallel-bedded, medium-grained sandstones (S_3; $T_{a-d,e}$), representing lobe deposits *sensu* Mutti & Normark (1987, 1991) (plate 2.8; *detailed analysis: chapter 2.4.3*). They are interbedded with finer-grained, thinner-bedded units of much lower sand/shale ratio of lobe fringe / interlobe origin *sensu* Mutti (1977) respectively. Contacts between the lobes and associated facies are mostly transitional resulting from lobe migration. Towards the top, lobe fringe deposits become increasingly more common.
Palaeocurrents point to a general NE transport direction.

E3) The top 110 m are dominated by noticeably finer-grained and thinner-bedded deposits characterised by a progressive upward decrease in the sand/shale ratio (ave. 3 - 1). Typically, 3-8 (max. 35) cm thick, fine-grained sandstones ($T_{b,c-d,e}$) are interbedded with 1-4 cm thick siltstones forming a thick, relatively monotonous unit especially towards the top. The sediments represent fan fringe deposits. The stratigraphic top of the Cingöz Formation is partly eroded into by Quaternary gravels partly not exposed, thus not permitting to determine the exact thickness of this unit. However, the recorded presence of Güvenç shales further upsection, suggests a possible maximum thickness of approximately 280 m of unit E3.

2.2.2.3 Lithologic and biostratigraphic correlations

Correlation between the individual sections proves difficult. This results from i) abundant faulting, ii) vast, heavily vegetated areas between the sections resulting in an "information gap" and iii) incomplete biostratigraphic data sets.
Deposits of the lowermost western section (W1) can be physically traced into the main fan area (study area 3; fig. 2.10, 2.11) which is interpreted to laterally correspond to the lowermost proximal lobe zone (C6) of the central fan section. The palaeocurrent pattern confirms the W1 sediments to be derived from this central fan area. Apart from this relationship, no direct lithologically-based correlations can be carried out.

The biostratigraphic data permits to tie most of the sections of the E-Fan into a temporal framework. During the incomplete (?) foraminiferal Praeorbulina glomerosa curva zone (late Burdigalian; Gürbüz 1993; Cronin *et al.* 2000) [*], 730 m of sediments were deposited in the western section and 420 m in the central section. The lower boundary of this zone, however, is most likely to be incorrect, i.e. is expected to be lower, especially in the central section. Sedimentation was absent in the eastern section. During the foraminiferal Orbulina suturalis zone (Langhian; Gürbüz 1993; Cronin *et al.* 2000) major changes in depositional style occur (fig. 2.11). A 7.8-fold sediment increase from 250 m of dominantly shales in the west to 2000 m of dominantly lobe sandstones and associated deposits in the central area are present. Palaeocurrent indicators generally point to the S-SE.
Cronin *et al.* (2000) found that during the Praeorbulina glomerosa curva and the lower part of the Orbulina suturalis zones, Kaplankaya slope sediments were deposited in the eastern part of the E-Fan. Here, the deposition of the turbiditic Cingöz Formation sets in during the Orbulina suturalis zone. Thus making the whole eastern section (section E) younger than most of the central and western section.
The foraminiferal Globorotalia mayeri zone marks the top of the E-Fan succession, with 110 (section W) and 100 m (section C) respectively. The biostratigraphic data for the eastern section (section E) are missing, however, equally little sedimentation is likely to have occurred.
Further implications of the differing biostratigraphic dating on the fan model are discussed in chapters 2.5 – 2.7.

2.3 Geometry of the fan - slope contact

Excellent exposures of the Karaisali reefal complex, Kaplankaya slope and the Cingöz clastic deep-water system reveal the complex stratigraphic and geometric relationships between the three systems. The reefal complex and slope system laterally interfinger; they are initially older, however, towards their upper parts coeval with the encroaching clastic turbidite system (Yetiş & Demirkol 1986; Nazik & Gürbüz 1992; Gürbüz 1993; Yetiş *et al.* 1995). Active slope progradation during times of Cingöz fan deposition leading to interfingering slope and fan deposition were recorded by Satur (1999), Cronin *et al.* (2000) and in this study (*chapter 2.2*). Cronin's *et al.* (2000) recent study indicates that slope thickness and gradient vary considerably along its ~ 60 km Cingöz-lateral extent due to slumping and mass wasting within the slope formation resulting from instability.
Fan-slope contacts are exposed at a number of locations along the north-western and north-eastern E-Fan margin (fig. 2.10: study areas 1 & 2). The observed contacts were differentiated into three discrete types, two of which represent pinch-out of fan sediments against the slope while the third emphasises an active fan-slope relationship.

2.3.1 Contact relationships

i) pinch out: onlap termination (unconformable, non-erosive contact) (fig. 2.12a):

This type of fan-slope contact can be readily observed along both margins. It is characterised by i) gradual thinning of individual beds and larger sediment packages against the slope, ii) progressive fining and iii) relatively thin slumped units (dm to m scale) with the slump folds pointing away from the slope (fig. 2.13; 2.14).
The pinch-out of fan deposits involves different hierarchies of scale. Figures 2.14 and 2.15 show that individual beds (cm to m-scale) as well as thicker sandstone packages (m to 10s of m scale) pinch-out. Slope gradients may vary considerably. While in the east (fig. 2.15) the slope exhibits a low, approximately 2° angle, in the west turbidites onlap an 8° steep slope (plate 3.1).
Sediments at the eastern fan-slope contact (fig. 2.14) exhibit a high amount of synsedimentary dewatering structures (dish structures), destroying much of the primary sedimentary structures. Rapid deposition and

[*] Toker *et al.* (1998) put the depositional age of the Cingöz Formation from early-middle Miocene (Langhian) to middle Miocene (Serravallian) based on calcareous nanoplankton, this age Satur (1999) appears to have used in his recent study, while Nazik & Gürbüz (1992), Gürbüz (1993) and Cronin, Gürbüz, Hurst & Satur (2000) utilise the foraminiferal biozones which give a late Burdigalian to Serravallian depositional age for the Cingöz Formation.

sediment overload typically result in dewatering (Nichols *et al.* 1994). However, Cronin *et al.* (2000) suggest creep or slurring of sandstone beds responsible for dewatering in such a setting.
The few palaeocurrent data indicate a broad scatter of current directions, diverging up to 60° (fig. 2.14). Transport directions in the distal lobe setting are largely axial, i.e. slope parallel. However, here transport appears to be directed obliquely to the laterally confining palaeoslope. It has been shown that subsequent deflection of turbidity currents is likely to occur (Pickering & Hiscott 1985; Kneller *et al.* 1991; Sinclair 1994), but the sparse data set does not conclusively support this assumption. This type of relationship is well known from other deep-water clastic systems such as the late Eocene Annot Sandstone of S-France (Ravenne 1992; Hurst *et al.* 1999) and the Tertiary Cengio Turbidite System (Cazzola *et al.* 1985). Hurst *et al.* (1999) assign onlap termination to down-system pinchout and attribute it to a lack of confinement of flow, however, oblique lateral confinement by the slope is present here (fig. 2.12a). Cronin *et al.* (2000) found this down-system onlap termination to exist further to the NE of the eastern study area, where turbidites onlap a low-gradient west-facing slope indicating restriction in basin accommodation.

ii) pinch out: infill (unconformable, non-erosive contact) (fig. 2.12b):

Infill *sensu* Hurst *et al.* (1999) involves a more abrupt termination of fan deposits against the slope which is characterised by a more sudden thickness decline and relatively little change in grain size. Along the NW but particularly the NE margin (2b of fig. 2.10), this type of contact features steep-angled and/or stepped geometries (fig. 2.12b; plate 2.2; 2.3) These geometries are probably generated by an irregular slope topography which allows fan sediments to accumulate in "slope pockets".

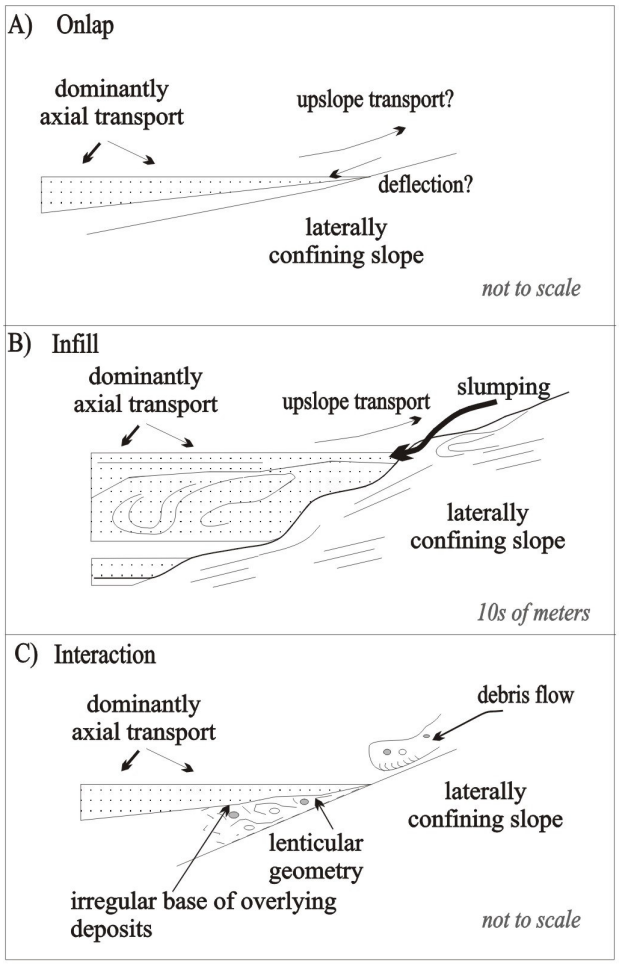

Figure 2.12: Schematic diagram showing the range of contact relationships encountered in the E-Fan. A and B represent different types of pinch out terminations.

The underlying slope sediments (plate 3.4) show abundant low angle unconformities believed to result from synsedimentary sliding of the slope deposits triggered by either high sedimentation rates, oversteepening of the slope and/or seismic activity thus producing the complex slope morphologies observed (Normark *et al.* 1993; Mulder & Cochonat 1996; Reading 1996; Cronin *et al.* 2000). These pockets may be anything from a few metres to 10s of metres in length and height (plate 3.2; 3.4), which are subsequently infilled by fan turbidites. Along the NE margin, abundant calcite harnishes were observed. They probably line synsedimentary glide planes which may be responsible for generating steep slope gradients. These gradients may be up to 24° (plate 3.4) and such steep slopes may promote sediment failure (Normark & Piper 1991).
Slumping and sliding involving individual beds or thicker fan-sediment packages commonly exist, but are particularly conspicuous in the NE, where metre-thick slumped packages are present (plate 3.4), infilling slope-pockets and/or occuring close to these. Muck & Underwood (1990) demonstrated that a considerable amount of upslope transport and deposition of turbidites can be expected when flows hit barriers, in this case the laterally confining slope. This may account for the deposition of fan sediments above the "active" depositional fan surface within the basin, their subsequent down-slope slumping and overlying by aggrading fan sediments.
The vertical and lateral changes within turbidites associated with infill geometries appear to be a

direct result of the underlying complex slope morphology where flow confinement results in steep pinch out relationships. Slumping and sliding of the underlying slope and of turbiditic fan sediments indicate an active fan margin environment.

iii interaction slope/shelf and fan sediments (fig. 2.12C)

Along the NW margin of the E-Fan (base of section W; chapter 2.2.2), another type of "active" fan-slope relationship is present (fig. 2.12C).
Log A (fig. 2.13) shows that fan turbidites are preceded by thick, lenticular debrites rich in lime- and siltstones as well as well-rounded, ophiolitic pebbles, passing upward into a thin succession of lenticular mixed pebbly – granule clastic and calcareous turbidites (plate 3.5, 3.6). These deposits appear to be confined to small channel-like fairways or slope gullies *sensu* Surlyk (1987) where erosion and filling are likely to be closely related processes. The slope gully fill is overlain by laterally more extensive sandstone beds rapidly terminating against a steep-angled (~ 15°) slope (infill-type; "marker bed"; fig. 2.13: Log B). Palaeocurrents indicate the clastic turbidites to derive from the NE-E, from the main fan area, while the underlying debrite and mixed turbidites were shed from the N of the shelf/slope. Stratigraphically upward lenticular, shelf/slope-derived debrites appear localised. Succeeding fan turbidites onlap their irregular topography (*chapter 2.2: Section W1/2*).

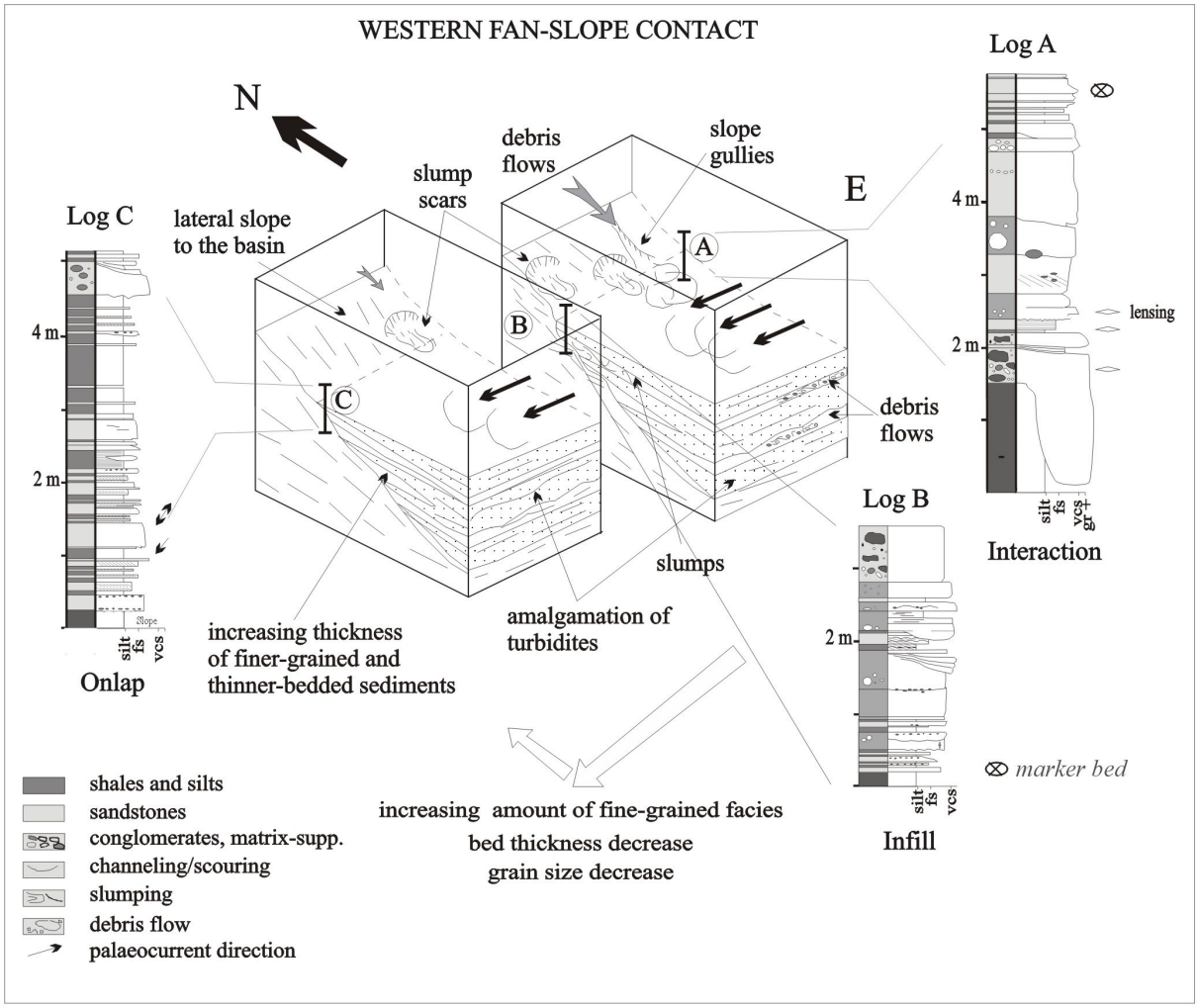

Figure 2.13: Schematic diagram showing the fan - slope contact along the north-western margin of the E-Fan. The type of contact varies from active fan-slope relationship with shelf/slope-derived debrites and calcareous turbidites to infill and onlap pinch out of fan deposits against the slope (location 1 of fig. 2.10.). Distance between logs: A - 50 m - B - 400 m - C.

Downcurrent, onlap termination of progressively finer-grained fan turbidites with only occasional slope-derived debrites higher up in the section was observed (fig. 2.13: log C). Up-current, towards the main fan

area and channel 4, slope-derived sediments are increasing in their frequency especially before or during onset of the fan encroachment. Small conglomeratic and/or debrite infilled bypass channels, showing accretion-like features, lensing, wedging and compensation features are occasionally present. The debrite clast content shows great similarity with the conglomeratic channel 4 deposits (*pers. comm.* Satur 1997) but with a much higher marly shale and shelfal limestone content.
Instability due to overloading/oversteepening and/or tectonic activity resulted in mass wasting of slope and shelf material just before and during the encroachment of the clastic turbidite system. On the one hand, it leads to the complex slope morphology prior to fan deposition with slump scars, varying gradients and slope gullies resulting in the observed contact geometries. On the other hand, slope instability, which appears to be greatest close to the fault-bounded channel 4, resulted in frequent debris flows and mixed turbidites coming from the shelf/slope interfingering with fan deposition. The debrite content suggests i) overspilling currents from the closeby, choked (?) channel 4 entraining shelf- or slope sediment or ii) other possibly fan delta-derived debrites deposited (?) at the upper shelf-break prior to its remobilisation due to oversteepening / seismicity and entrainment of shelf and slope sediments.

2.3.2 Western versus eastern fan-slope contacts

Slope stability and morphology profoundly influence the geometry of the fan-slope contact.

The western margin exhibits an active fan-slope relationship with abundant shelf/slope derived debrites and mixed turbidites closest to channel 4 changing to infill and onlap pinch-out (plate 3.1-2, 5-6) in a downcurrent, westward direction (fig. 2.13; table 2.3). The Cingöz turbidites display a progressive change by i) decrease in the sand/shale ratio, ii) dramatic decrease in grain size, iii) overall bed thickness decrease, iv) increase in amount of interbedded finer-grained facies and v) transition from proximal partly channelized to fan fringe deposition (fig. 2.13; table 2.3).

Logs	Debris flow : Sand : shale	Grain size	Bed thickness	Erosional contacts	Geometries	Depositional environment
Log A	0.9:1:0.1	cs-gr	ave. 80 cm	abundant	lensing, pinch-out (infill)	Channel influenced?, lobe fringe deposits
Log B	0.4:1:0.2	cs-vcs	ave. 60 cm	common	pinch-out (infill)	lateral lobe fringe?, fan fringe
Log C	0.2:0.6:1	vfs-fs	ave. 25 cm	rare	pinch-out (onlap)	lateral fan fringe

Abbreviations: gr=granule, vcs= very coarse sand, cs=coarse sand, fs=fine sand, vfs=very fine sand, ave=average

Table 2.3: Variations along the western fan-slope contact (fig. 2.13). Distances between logs: A – 50 m – B – 400 m – C.

The mean grain size of the sandstones along the NW margin is considerably coarser than that of the NE margin (*see below*), although the studied section is generally dominated by thick successions of finer-grained facies, where siltstones are commonly interbedded with relatively thin-bedded, coarse to pebbly units and occasional debris flows (*chapter 2.2*). Contemporaneous slope instability resulting in frequent mass wasting events is characteristic. Slumping of semilithified Cingöz deposits was not observed.

The deposits at the eastern margin are interpreted to be lobe and lobe-fringe deposits (*chapter 2.2*; table 2.4). The fan sediments onlap an approximately 2° angled slope (fig. 2.14, 2.15), however, locally steeper gradients (up to 24°) were recognised due to irregular slope topography resulting from sliding and slumping of underlying slope segments.
The palaeocurrent indicators point to a NE-ENE transport direction, which is nearly parallel to the confining slope. Oblique upslope transport and subsequent rebound of turbidity currents is likely to have occurred. Sand-rich sandstone packages (Log A) laterally thin, exhibiting a more distinct asymmetric, coarsening-upward signature and containing a higher mudstone content (Log B). These developments have also been observed elsewhere (e.g. Annot Sandstone: Sinclair 1994).

Logs	Sand : shale	Grain size	Bed thickness	slumping	Geometries	Depositional environment
Log A	1 : 0.5	ms	ave. 40 cm	common-axis away	pinch-out (onlap)	lobe- and interlobe deposits
Log B	1 : 0.9	fs	ave. 15 cm	common-axis away	pinch-out (onlap)	lobe - and interlobe deposits

Abbreviations: ms=medium sand, fs=fine sand, ave=average

Table 2.4: Variations along the eastern fan-slope contact (fig. 2.14, 2.15). Distances between logs: 200m.

Some of the studied sections along the NE-margin are within a large fault-displaced slab of Cingöz Formation and it is not possible to tie them into the E-Fan framework (Ünlügenç 1993; *pers. comm.* Ünlügenç 1996). These are the sections which exhibit the marked infill relationships, the thick slumped units of lobe and associated deposits infilling the underlying irregular slope topography.

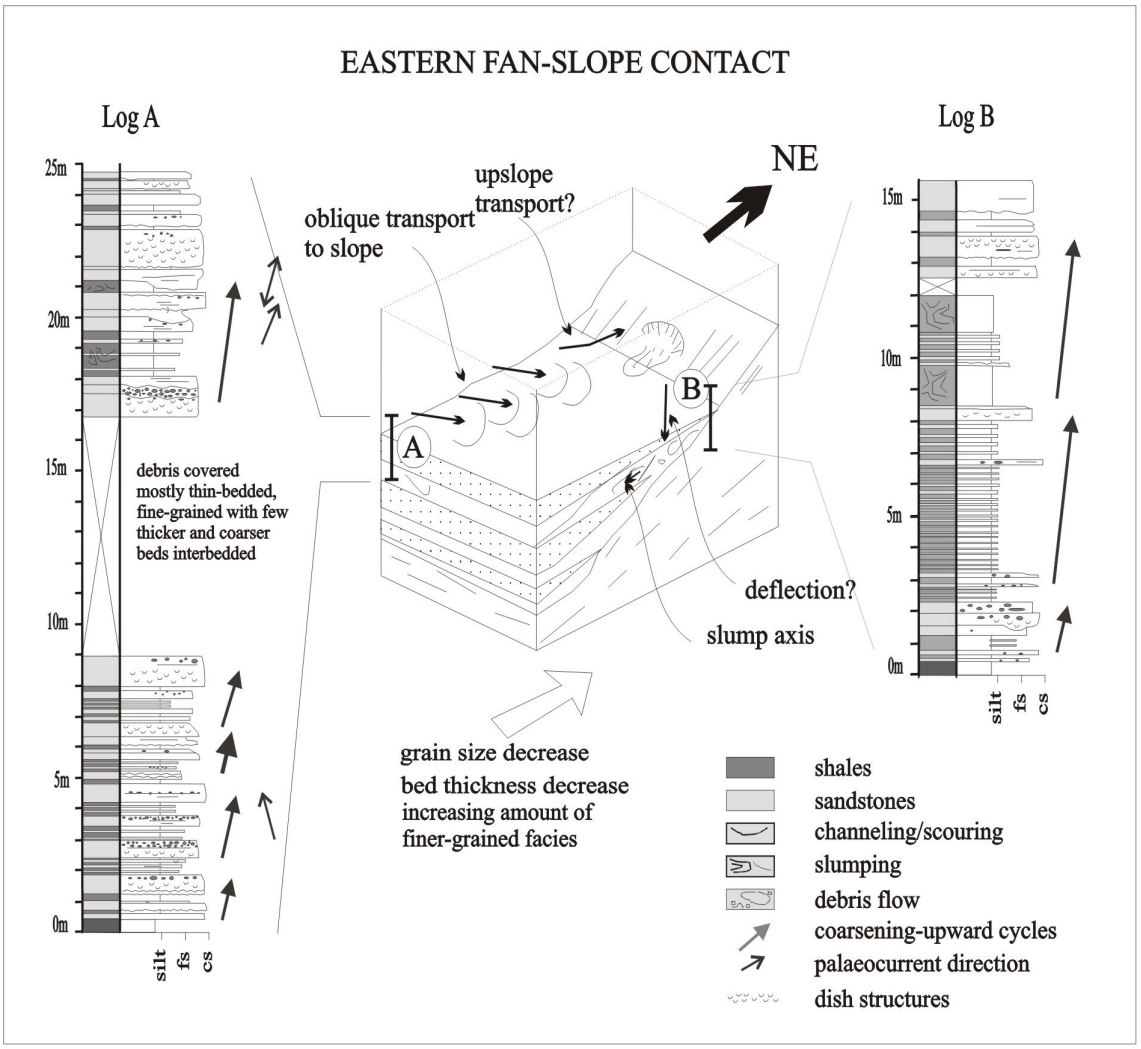

Figure. 2.14: Schematic diagram showing fan deposits onlapping the slope exposed in a cutbank north of Egner, E-Fan (Location 2a of fig. 2.10). The vertical fan development in both locations shows thickening and coarsening upward from the fan-slope contact. Laterally, marked grain size and bed thickness decrease towards the slope (A to B) takes place while the amount of finer-grained facies increases. The slope has an approximate gradient of 2°. Distance between logs: ~200 m.